Thermochimica Acta, 23 (1978) 135–144
© Elsevier Scientific Publishing Company, Amsterdam – Printed in The Netherlands

A STUDY OF THE FORMATION OF $LiNbO_3$ IN THE SYSTEM Li_2CO_3–Nb_2O_5

SHIRO SHIMADA, KOHEI KODAIRA AND TORU MATSUSHITA
Department of Applied Chemistry, Faculty of Engineering, Hokkaido University, Sapporo 060 (Japan)
(Received 21 March 1977)

ABSTRACT

The formation process of $LiNbO_3$ in the system Li_2CO_3–Nb_2O_5 was discussed from the results of non-isothermal or isothermal TG experiments and X-ray analysis. The mixture Li_2CO_3 and Nb_2O_5 in mole ratios of 1:3, 1:1 or 3:1 was heated at a rate of 5°C min^{-1} or at various temperatures fixed in the range 475 to 677°C. If the system has a composition of $Li_2CO_3 + 3Nb_2O_5$ or $3Li_2CO_3 + Nb_2O_5$, the reaction between Li_2CO_3 and Nb_2O_5 proceeds with CO_2 evolution to form $LiNbO_3$ at ca. 300–600°C, but Nb_2O_5 or Li_2CO_3 remains unreacted. A composition of $Li_2CO_3 + Nb_2O_5$ gives $LiNbO_3$ at 300–700°C. The diffusion of Li_2O through the layer of $LiNbO_3$ is rate-controlling with an activation energy of 51 kcal mol^{-1}. The reaction between $LiNbO_3$ and Nb_2O_5 gives $LiNb_3O_8$ at 600–700°C. At 700–800°C, a slight formation of Li_3NbO_4 occurs by the reaction between $LiNbO_3$ and Li_2O at the outer surface of $LiNbO_3$ and the Li_2O component of Li_3NbO_4 diffuses toward the boundary of the $LiNb_3O_8$ layer through the $LiNbO_3$ layer. The single phase of $LiNbO_3$ is formed above 850°C.

INTRODUCTION

Lithium niobate ($LiNbO_3$) is a ferroelectric material having a high Curie point. Single crystals of $LiNbO_3$ are of importance as electro-optic materials[1]. Sintered ceramics of $LiNbO_3$ are of great interest because they have many applications in the field of dielectrics. $LiNbO_3$ is formed by the solid-state reaction between Li_2CO_3 and Nb_2O_5. The preparation of reactive powder of $LiNbO_3$ with homogeneous composition is important to obtain its dense sintered ceramics. Therefore, it is necessary to study the formation of $LiNbO_3$ by the reaction between Li_2CO_3 and Nb_2O_5. In this paper, we elucidated the mechanism for the formation of $LiNbO_3$ in the system Li_2CO_3-Nb_2O_5 with various compositions.

EXPERIMENTAL

The starting materials were niobium pentoxide (99.9% pure) and lithium carbonate (G.R. grade). The particle size of Nb_2O_5 for 400 particles was micro-

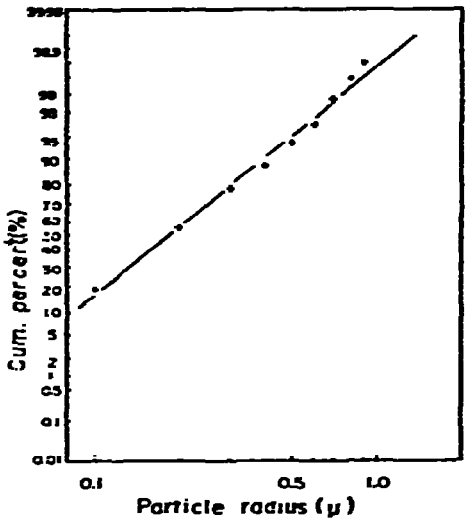

Fig. 1. Log normal probability graph of Nb_2O_5 particles size.

scopically determined in the range of 0.1–1.0 μ. Figure 1 shows the log probability plots of the size distribution of Nb_2O_5 particles. This indicates that the Nb_2O_5 particle sizes obey the log normal distribution. The Nb_2O_5 particles were approximately cylindrical in shape. By means of SEM, the particle size of Li_2CO_3 was found to be in the range 1.0–3.0 μ. The particles were approximately platy in shape. Powder of Nb_2O_5 and Li_2CO_3 was thoroughly mixed in a mortar with a pestle in the mole ratios of 1:3, 1:1, 3:1. The mixed powder was stored in a desiccator with silica gel.

The reaction between Nb_2O_5 and Li_2CO_3 was followed by a TG experiment. The TG experiment was carried out with an apparatus attached to a RMB-5V type microbalance (Shimazu Seisaku Sho), the accuracy of which corresponds to $\pm$ 1%. The mixed powder (ca. 30 mg) was lightly packed in a fused-silica basket (7 mm in diameter and 3 mm in depth) and it was suspended in a fused-silica tube (30 mm in diameter) through which dry air or nitrogen was allowed to flow at a rate of 20 ml min^{-1}. The reaction temperature was measured with a Pt–Pt/13%Rh thermocouple, being attached to the inside of the tube at the height of the basket. The non-isothermal TG experiment was carried out by heating at a rate of 5°C min^{-1} under flowing air. The isothermal TG experiment was carried out at various temperatures fixed in the range of 475 to 677°C under the same condition. The buoyancy correction was checked at elevated temperatures under flowing air. X-ray analysis was performed for the samples obtained by TG experiments. The DTA experiment was carried out with a Thermoflex apparatus (Rigaku-Denki). A heating rate of 10°C min^{-1} was applied. α-Al_2O_3 was taken as the standard material.

RESULTS

Figure 2 shows weight loss curves on heating of a mixed powder of Li_2CO_3

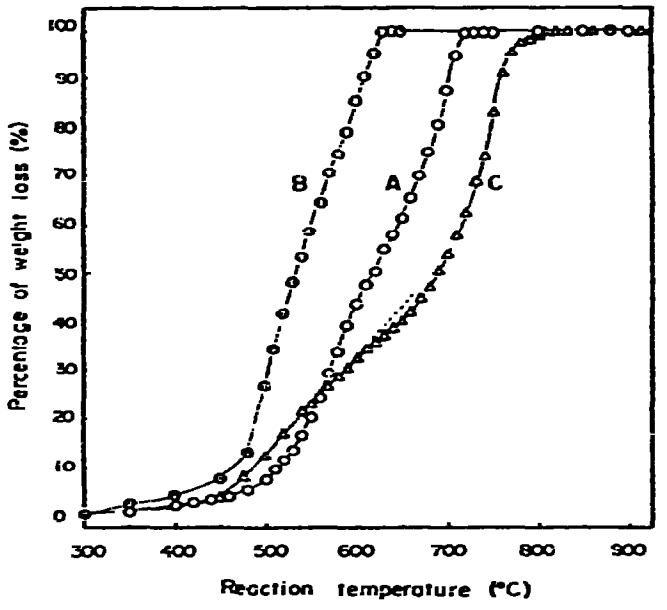

Fig. 2. Weight loss curves on heating the mixed powder of Li_2CO_3 and Nb_2O_5 in mole ratios 1:1 (curve A), 1:3 (curve B) or 3:1 (curve C). $\varnothing$ = 5°C min^{-1}, flowing air: 20 ml min^{-1}.

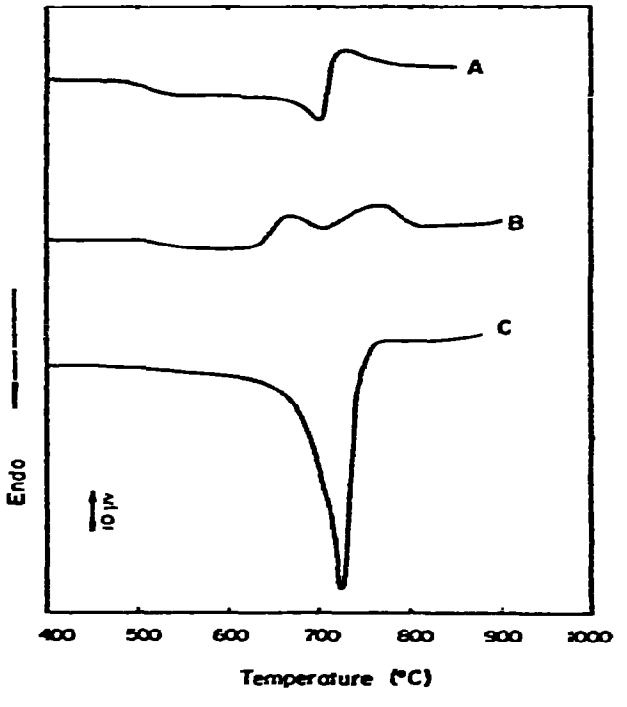

Fig. 3. DTA curves on heating the mixed powder of Li_2CO_3 and Nb_2O_5 in mole ratios 1:1 (curve A), 1:3 (curve B) or 3:1 (curve C). $\varnothing$ = 10°C min^{-1}, Pt-Pt/13%Rh thermocouple, static air. Sample weight; curve A: 339 mg, curve B: 452 mg, curve C: 348 mg.

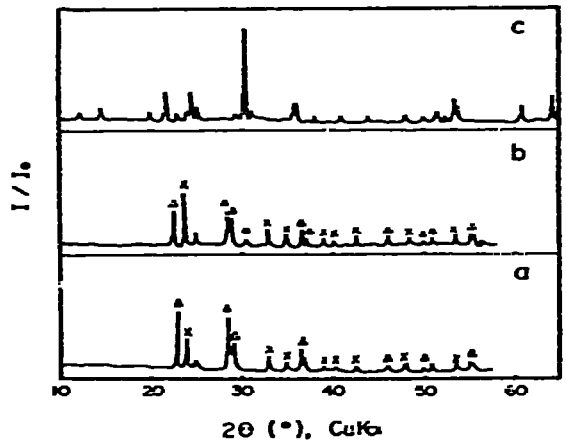

Fig. 4. X-ray diffraction patterns of samples heated to temperatures corresponding to points on TG curve using a composition of $Li_2CO_3 + 3Nb_2O_5$. △ = Nb_2O_5; × = $LiNbO_3$; ● = $LiNb_3O_8$. ∅ = 5 °C min^{-1}; (a) 560 °C, (b) 650 °C, (c) 880 °C.

and Nb_2O_5 in the mole ratios of 1 : 1 (curve A), 1 : 3 (curve B) or 3 : 1 (curve C) under flowing air. The ordinate corresponds to the percentage of the weight loss of CO_2 calculated from the amount of Li_2CO_3 contained in the mixed powder by use of the decomposition equation of Li_2CO_3: $Li_2CO_3 \rightarrow Li_2O + CO_2$. In curve A, the weight loss continues to increase from 300 °C, the degree of the increase falling slightly at ca. 600 °C and is completed at 720 °C. In curve B, it begins to occur at 300 °C, a rapid increase being observed from 480 °C and is completed at 630 °C. Curve C shows that there is an inflection point at ca. 600 °C, as indicated by the dotted line. The weight loss in curve C may proceed at two stages: the first at 300–600 °C and the second at 600–820 °C. Figure 3 shows DTA curves on heating of the mixed powder of Li_2CO_3 and Nb_2O_5 in the mole ratios 1 : 1 (curve A), 1 : 3 (curve B) or 3 : 1 (curve C). Curve A shows an endothermic peak at 470–720 °C and an exothermic peak at 720–800 °C. Curve B shows one endothermic peak at 500–640 °C and two exothermic peaks at 640–810 °C. Curve C shows one large endothermic peak in the range 470–780 °C.

Figure 4 shows the X-ray diffraction patterns of the samples heated to temperatures corresponding to points on the TG curve with a composition of $Li_2CO_3 + 3Nb_2O_5$. At 560 and 650 °C, the peaks for $LiNbO_3$ are observed, those for Nb_2O_5 remaining. The weak (410) reflection for $LiNb_3O_8$ is seen[2] at 650 °C. The single phase of $LiNb_3O_8$ is obtained at 880 °C. Fig. 5 shows the X-ray diffraction patterns of the samples heated to temperatures on the TG curve with a composition of $3Li_2CO_3 + Nb_2O_5$. The peaks for $LiNbO_3$ are observed, those for Li_2CO_3 and Nb_2O_5 remain at 600 °C. With a rise in reaction temperature at 700–870 °C, the peaks for $LiNbO_3$ are lowered and those[3] for Li_3NbO_4 are simultaneously increased. The single phase of Li_3NbO_4 is obtained at 910 °C. Figure 6 shows changes of the X-ray intensities for $LiNbO_3$, $LiNb_3O_8$, Li_3NbO_4 and Nb_2O_5 in the samples heated to temperatures on the TG curve when a system with a composition of Li_2CO_3 and Nb_2O_5 is used. $LiNbO_3$ increases continuously with a rise in reaction temperature. However, Nb_2O_5

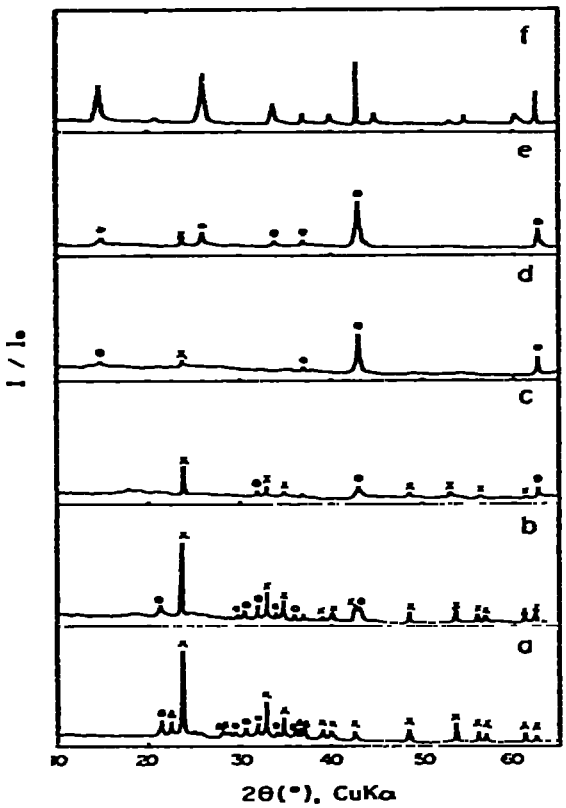

Fig. 5. X-ray diffraction patterns of samples heated to temperatures corresponding to points on TG curve using a composition of $3Li_2CO_3 + Nb_2O_5$. ○ = Li_2CO_3; △ = Nb_2O_5; × = $LiNbO_2$; ● = Li_3NbO_4. Ø = 5°C min^{-1}; (a) 600°C, (b) 700°C, (c) 740°C, (d) 790°C, (e) 870°C, (f) 910°C.

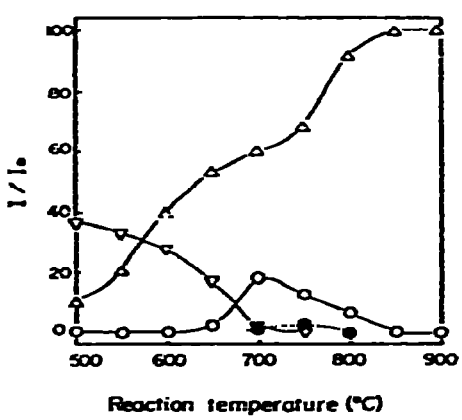

Fig. 6. Changes of X-ray intensities for Nb_2O_5, $LiNbO_2$, $LiNb_3O_8$ or Li_3NbO_4 in samples heated to temperatures corresponding to points on TG curve using a composition of $Li_2CO_3 + Nb_2O_5$. ▽ = Nb_2O_5(001); △ = $LiNbO_2$(012); ○ = $LiNb_3O_8$(410); ● = Li_3NbO_4(400). Ø = 5°C/min.

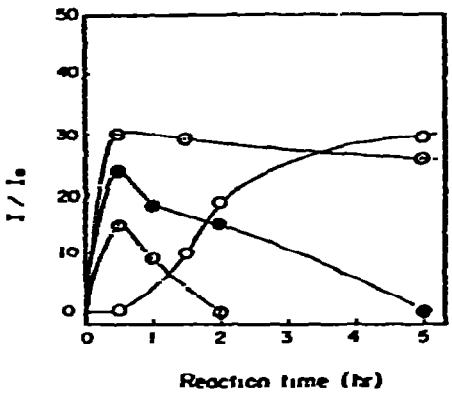

Fig. 7. Changes of intensities of (410) reflection for $LiNb_3O_8$ in samples with a composition of Li_2CO_3 + Nb_2O_5 heated at various temperatures. ○ — 600°C; ⊙ — 700°C; ● — 800°C; ⓘ — 900°C.

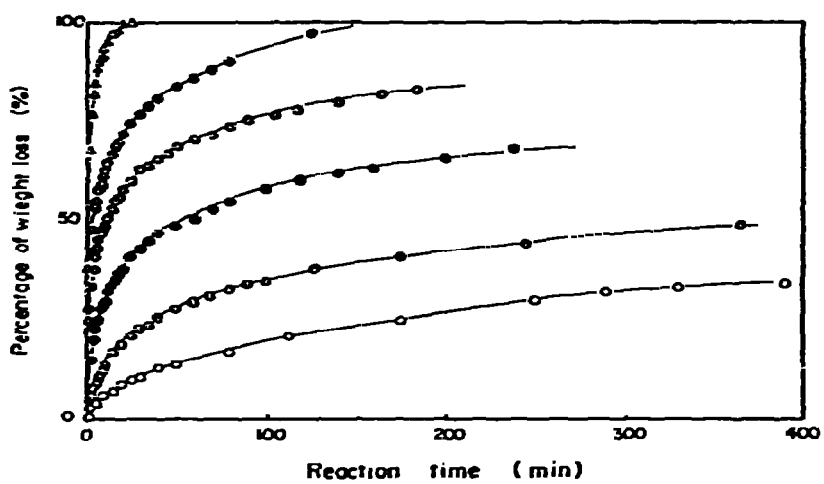

Fig. 8. Weight loss curves of the mixed powder of Li_2CO_3 and Nb_2O_5 in mole ratio 1:1. ○ — 475°C; ○ — 510°C; ● — 557°C; ⓘ — 606°C; ⊖ — 636°C; △ — 677°C.

continues to decrease and disappears at 750°C, which is close to the temperature of the complete weight loss determined in Fig. 2(A). $LiNb_3O_8$ begins to appear at ca. 600°C, reaches the maximum at 700°C and disappears at 850°C. The weak peak for Li_3NbO_4 is observed at 700–750°C. Figure 7 shows the X-ray intensity for $LiNb_3O_8$ in the samples heated at various temperatures in the range 600–900°C when a composition of Li_2CO_3 + Nb_2O_5 is used. $LiNb_3O_8$ increases continuously after 0.5 h at 600°C and decreases after 0.5 h at 700–900°C. It disappears after 5 h at 800°C or 2 h at 900°C.

Figure 8 shows weight loss curves of the mixed powder of Li_2CO_3 and Nb_2O_5 at temperatures in the range 475 to 677°C. The weight loss increases parabolically at each temperature.

DISCUSSION

In each composition, the amount of weight loss when the reaction was finished was consistent with that of CO_2 calculated from the complete decomposition of Li_2CO_3 (Fig. 2). This indicates that the weight loss on TG curves is due to CO_2 evolution. It is said[4] that Li_2CO_3 begins to decompose to Li_2O and CO_2 at 618°C. No weight loss was observed in the TG measurement of pure Li_2CO_3 up to ca. 500°C. There was little difference in the weight loss curves under the different atmospheres. The results of the X-ray analysis for the samples obtained by TG experiments (Figs. 4–6) showed the formation of lithium niobate ($LiNbO_3$, $LiNb_3O_8$ or Li_3NbO_4). These imply that CO_2 evolution is associated with the reaction between Li_2CO_3 and Nb_2O_5, resulting in the formation of lithium niobate.

With a composition of $Li_2CO_3 + 3Nb_2O_5$, CO_2 evolution started at 300°C, a rapid increase in its amount being observed from 480°C and was finished at 630°C (Fig. 2(B). The temperature range of 480–630°C coincides with that of the endothermic peak on DTA curve (Fig. 3(B). The results of the X-ray analysis showed the presence of $LiNbO_3$ at 560 and 650°C. Thus, it is concluded that the reaction between Li_2CO_3 and Nb_2O_5 proceeds endothermally with the formation of $LiNbO_3$ at 300–630°C. The presence of $LiNb_3O_8$ above 650°C is due to the further reaction between $LiNbO_3$ and Nb_2O_5: $LiNbO_3 + Nb_2O_5 \rightarrow LiNb_3O_8$. The formation of $LiNb_3O_8$ may exothermally proceed at the two stages, as shown in Fig. 3(B).

As described above, the reaction between $3Li_2CO_3$ and Nb_2O_5 proceeds at the two stages: the first at 300–600°C and the second above 600°C. The reaction at the two stages accompanies the large endothermic effect, as shown in Fig. 3(C). When the first stage was finished at 600°C, $LiNbO_3$ was formed (Fig. 5). The percentage of CO_2 evolution reached 34% at 600°C. This indicates that the equimolecular reaction between Li_2CO_3 and Nb_2O_5 occurs to form $LiNbO_3$ at the first stage. Li_3NbO_4 was detected by X-ray analysis at 700°C. It is concluded that further reaction between $LiNbO_3$ and Li_2CO_3 occurs to form Li_3NbO_4 at the second stage.

With a composition of $Li_2CO_3 + Nb_2O_5$, CO_2 evolution started at 300°C, the degree of its increase falling slightly above 600°C and was finished at 720°C (Fig. 2(A). The results of X-ray analysis (Fig. 6) showed the increase of $LiNbO_3$ with simultaneous decrease of Nb_2O_5 at 500–700°C. On the other hand, $LiNb_3O_8$ began to form at 600°C and disappeared at 850°C through the maximum at 700°C. This indicates that the reaction between Li_2CO_3 and Nb_2O_5 occurs to form $LiNbO_3$ with evolution of CO_2 at 300–700°C and the further reaction between $LiNbO_3$ and Nb_2O_5 results in the formation of $LiNb_3O_8$ at 600–700°C. $LiNb_3O_8$ in addition to $LiNbO_3$ remains in the reaction product (Fig. 6), even after complete evolution of CO_2 at 720°C. Thus, there must be an amount of Li_2O in it because the equivalent amount of Li_2CO_3 and Nb_2O_5 is added. This may be consumed for the Li_3NbO_4 formation by the reaction between $LiNbO_3$ and Li_2O. This is supported by the formation of Li_3NbO_4 observed at 700–750°C. Accordingly, it is thought that the $LiNbO_3$ formation above 700°C is due to the reaction between $LiNb_3O_8$ and Li_3NbO_4.

DTA curve 3-A can be explained as follows: an endothermic peak is due to CO_2 evolution and an exothermic peak corresponds to $LiNb_3O_8$ formation due to the overlap of the endothermic peak with the exothermic peaks corresponding to those of curve 3-B.

As described above, the weight loss in Fig. 8 is associated with CO_2 evolution, i.e., $LiNbO_3$ formation. $LiNb_3O_8$ increased continuously at 600°C after 0.5 h (Fig. 7), the condition of which corresponds nearly to the fractional conversion $F = 60$–70% of $LiNbO_3$ formation in Fig. 8. In the range $F = 0$–60% without $LiNb_3O_8$ formation, kinetic data of Fig. 8 were treated with various equations[5–8]. As a result, it was found that the kinetic data fit best to Jander's equation[5], in spite of some deviation. The main cause for the deviation is considered to be due to the wide size distribution of Nb_2O_5 particles, as shown in Fig. 1. Gallagher[9] has evaluated the effect of the size distribution of particles on the reaction rate by use of the Serin-Ellickson equation. We similarly applied his method to the data in Fig. 8 by introducing the size distribution of particles into the Jander's equation. The equation is expressed by

$$[1 - (1 - F)^{1/3}]^2 = kt \tag{1}$$

$$k = 2DC_0/r^2 \tag{2}$$

$$F = 1 - \left(1 - \sqrt{2DC_0t/r^2}\right)^3 \tag{3}$$

where k = rate constant, t = reaction time, D = diffusion coefficient, C_0 = concentration of reactant at the interface, and r = particle radius. The Nb_2O_5 particles were distributed according to the log normal distribution (Fig. 1). It is necessary to evaluate the fractional conversion about each of particles with the log normal distribution and then compute the total fractional conversion of all the reacted particles. The total fraction conversion, F, is expressed by[9, 10]

$$F = \sum_{m=-\infty}^{m=\infty} F_m(\delta V/V)_m = \sum_{m=-\infty}^{m=\infty} [1 - \left(1 - \sqrt{G/\sigma_g^{2m/L}}\right)^3](\delta V/V)_m \tag{4}$$

where F_m = the fractional conversion in a particle with a radius equal to that of the m th slice on the log normal distribution, $(\delta V/V)_m$ = the volume fraction in the m th slice, $G = 2DC_0t/(r_g')^2$ (r_g' = geometric mean radius by volume), σ_g = geometric standard deviation by volume, L = the number of slices into which the interval log σ_g is divided ($L = 5$ in this case), m = a number: -14.5, . . ., -1.5, -0.5, 0, 0.5, 1.5, . . ., 14.5, for $L = 5$. In eqn (4), the standard deviation range of $+3\log\sigma_g$ to $-3\log\sigma_g$ is put on both sides of the mean. From Fig. 1, the values of both r_g and σ_g are graphically evaluated[11]: $r_g = 1.8$ and $\sigma_g = 2.0$. If a value of G is evaluated from eqn (4) for a measured value of F, Jander's curves are computed over a wide range of values of σ_g on a reduced time scale[12] and can be compared with the experimental data on the same scale. However, it is impossible to compute G directly from F. Hence, the G value corresponding to a given value of F in $F = 0$–0.70 was computed within an error less than ± 0.002 of F value by trial and error on a FACOM230-60/75 computer.

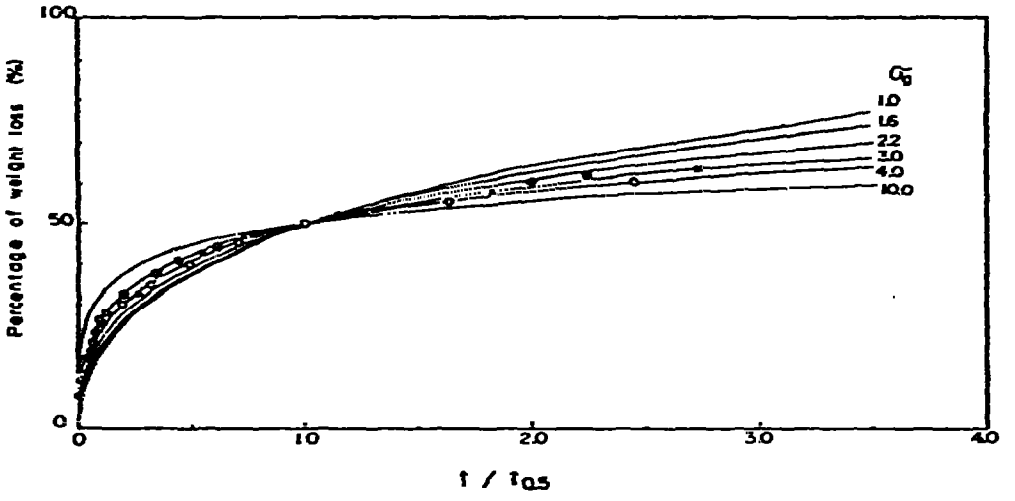

Fig. 9. Computed Jander's curves on a reduced time scale as a parameter of σ_g and experimental points of Fig. 8 plotted on the same time scale. Experimental points: O = 510°C; O = 557°C; × = 606°C; ● = 636°C.

Figure 9 shows the experimental points of Fig. 8 plotted on a reduced time scale and the Jander's curves computed on the same scale as a parameter of σ_g by use of the above computed values of F and G. The curve for $\sigma_g = 1$ corresponds to the case of uniform particle size. A comparison of the experimental points with the Jander's curves for a variety of σ_g indicates that $LiNbO_3$ formation can be described by Jander's equation having the particle size distribution of Nb_2O_5 in $\sigma_g = 3.0$ to 4.0. The discrepancy of the above σ_g value with $\sigma_g = 2.0$ determined from Fig. 1 may result from a difference in the shape of particles[9]: the particle size in the case of Fig. 8 is assumed to be spherical, but is cylindrical in reality. The k constants were obtained in both cases of $\sigma_g = 3.0$ and 4.0 and the value of activation energy from the plots of log k against $1/T$ was determined to be 51 kcal mol^{-1}. The SEM observation showed that the reacted powders at 750°C in Fig. 2(A) are cylindrical in spite of a reduction in size. On the contrary, the plate-like particles which have the same shape as Li_2CO_3 particles were not observed. This suggest that the reaction between Li_2CO_3 and Nb_2O_5 proceeds by the diffusion of Li_2O through the formed layer of $LiNbO_3$.

The mechanism for $LiNbO_3$ formation in the system Li_2CO_3–Nb_2O_5 is summarized as follows. With a composition of $Li_2CO_3 + 3Nb_2O_5$ or $3Li_2CO_3 + Nb_2O_5$, the equimolecular reaction between Li_2CO_3 and Nb_2O_5 proceeds with CO_2 evolution to form $LiNbO_3$ at ca. 300–600°C, but Nb_2O_5 or Li_2CO_3 remains unreacted. The reaction of a composition of $Li_2CO_3 + Nb_2O_5$ can be illustrated by Fig. 10. At 300–700°C, the reaction between Li_2CO_3 and Nb_2O_5 occurs to form $LiNbO_3$. The diffusion of Li_2O through the layer of $LiNbO_3$ is rate-controlling with the activation energy of 51 kcal mol^{-1}. At 600–700°C, $LiNb_3O_8$ results from the reaction between $LiNbO_3$ and Nb_2O_5. CO_2 evolution is finished at 720°C. Near this temperature, an excess amount of Li_2O remains at the outer surface of $LiNbO_3$. Li_2O reacts with

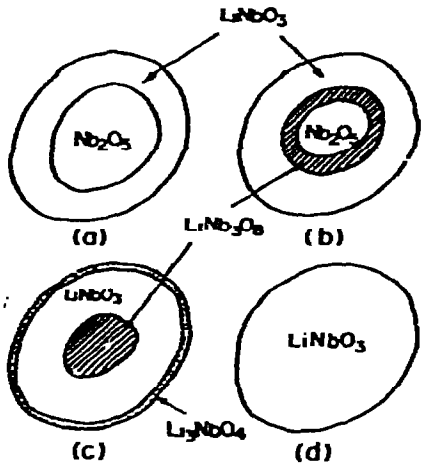

Fig. 10. Schematic representation of a powder reaction of a composition of $Li_2CO_3 + Nb_2O_5$. (a) 300–600°C; (b) 600–700°C; (c) 700–850°C; (d) above 850°C.

$LiNbO_3$ to form Li_3NbO_4. At 700–850°C, the Li_2O component of Li_3NbO_4 diffuses toward the boundary of the $LiNb_3O_8$ layer through the $LiNbO_3$ layer. The single phase of $LiNbO_3$ develops above 850°C.

ACKNOWLEDGEMENTS

We express our thanks to Dr. H. Ochiai, Department of Machinery Design, for helpful discussion in computer programming. Financial support for this work was given by The Sakkokai Foundation.

REFERENCES

1 G. E. Peterson, A. A. Ballman, P. V. Lenzo and P. M. Bridenbaugh, *Appl. Phys. Lett.*, 5 (1964) 62.
2 M. Lundberg, *Acta Chem. Scand.*, 25 (1971) 3337.
3 G. Blasse, *Z. Anorg. Allg. Chem.*, 326 (1963) 44.
4 *Nippon Kagaku Kai Hen*, Kagakubinran Oyohen, 1973, p. 169.
5 W. Jander, *Z. Anorg. Allg. Chem.*, 163 (1927) 1.
6 K. J. Laidler, *Chemical Kinetics*, McGraw-Hill, New York, 1964, p. 316.
7 B. Serin and R. J. Ellickson, *J. Chem. Phys.*, 9 (1941) 742.
8 A. M. Ginstling and B. I. Brounshtein, *J. Appl. Chem.*, 23 (1950) 1327.
9 K. J. Gallagher, in G. H. Schwab (Ed.), *Reactivity of Solids*, Amsterdam, 1965, p. 192.
10 H. Herdan, *Small Particle Statistics*, Elsevier, Amsterdam, 1953, p. 113.
11 H. Herdan, *Small Particle Statistics*, Elsevier, Amsterdam, 1953, p. 132.
12 J. H. Sharp, G. W. Brindley and B. N. Ivarahari Achar, *J. Am. Ceram. Soc.*, 49 (1966) 379.